

Hole Dynamics in the Orthogonal-Dimer Spin System

Yasuhiro Saito, Akihisa Koga and Norio Kawakami

Department of Applied Physics, Osaka University, Suita, Osaka 565-0871, Japan

(Received November 21, 2018)

The dynamics of a doped hole in the orthogonal-dimer spin system is investigated systematically in one, two and three dimensions. By combining the bond-operator method with the self-consistent Born approximation, we argue that a dispersive quasi-particle state in the dimer phase is well defined even for quasi-two-dimensional systems. On the other hand, a doped hole in the plaquette-singlet phase hardly itinerates, forming an almost localized mode. We further clarify that although the quasi-particle weight in the dimer phase is decreased in the presence of the interchain coupling, it is not suppressed but even enhanced upon the introduction of the interlayer coupling.

KEYWORDS: SrCu₂(BO₃)₂, Orthogonal-dimer, Shastry-Sutherland model, self-consistent Born approximation, bond operator

1. Introduction

Recently, low-dimensional quantum spin systems with frustration have attracted much interest. Among them, a quasi-two-dimensional (2D) spin gap compound SrCu₂(BO₃)₂^{1,2)} is outstanding in its unique features. The crystal structure of the compound is such that Cu²⁺ ions with spin $S = \frac{1}{2}$ are located on the orthogonal-dimer lattice, resulting in the characteristic magnetic properties.³⁻⁷⁾ Miyahara and Ueda⁸⁾ pointed out that the orthogonal-dimer lattice is equivalent to the square lattice with some diagonal bonds, which is referred to as the Shastry-Sutherland model.⁹⁾ (See Fig. 1) The system has been providing a variety of interesting issues,¹⁰⁾ e.g. quantum phase transitions,^{8,11-19)} unique triplet excitations,^{12,20-25)} magnetization plateaus.^{14,20-22,26-29)} It was found that the ground state of the compound SrCu₂(BO₃)₂ is in the dimer phase close to the quantum phase transition point.⁸⁾ Therefore, the application of the magnetic field^{1,3)} or the pressure,⁷⁾ could trigger a quantum phase transition. Also, some reports claimed that the compound SrCu₂(BO₃)₂ has a rather large interlayer interaction to explain the experimental data such as the susceptibility and the specific heat.^{12,30)}

The study of a single hole doped into the above orthogonal-dimer system is important,³¹⁾ since its dynamics determines the profile of the photoemission spectrum. In comparison with the extensive theoretical investigations of static quantities, such one-particle spectral properties have not been studied systematically, except for Vojta's work on the dimer phase of the 2D Shastry-Sutherland model.³¹⁾ In particular, it is desirable to clarify how the interlayer coupling, which turns out to be important for the static quantities, affects the photoemission spectrum. Moreover, such investigations of a doped hole may provide a starting point to study the system with finite density of holes, which may be realized by the chemical substitution of some elements. Although simple substitution of Zn ions for Cu ions results in localized magnetic moments,³²⁾ it is an interesting issue to realize a metallic orthogonal-dimer system experimentally.

Motivated by the above topics, we investigate the dynamics of a doped hole in the orthogonal-dimer system systematically in one, two and three dimensions. By means of the self-consistent Born approximation (SCBA)³³⁻³⁸⁾ with the bond-operator representation^{31,37-41)} and also the exact diagonalization (ED), we discuss how the characteristic orthogonal-dimer structure affects the motion of a doped hole.

This paper is organized as follows. In Sec. 2, we introduce the orthogonal-dimer spin system, which is relevant to describe the system of SrCu₂(BO₃)₂. In Sec. 3, we briefly summarize the bond operator representation for quantum spins, which is combined with the self-consistent Born approximation to treat a doped hole. This method is used for the analysis of the dimer phase, whereas the ED method is also employed to treat the hole dynamics in the plaquette phase. In Sec. 4, we study the dynamics of a doped hole systematically in one, two and three dimensional orthogonal-dimer systems, and clarify the role of the lattice geometry on the dynamics of a doped hole. A brief summary is given in Sec. 5.

2. model

We investigate the orthogonal-dimer spin model,^{12,42,43)} which is schematically drawn in Fig. 1. To deal with the system with a hole, we consider the following t - J Hamiltonian,

$$H = H_t + H_J, \quad (1)$$

$$H_J = \sum_{\kappa=1,4} J_{\kappa} \sum_{\langle i,j \rangle \in D_{\kappa}} \mathbf{S}_i \cdot \mathbf{S}_j \quad (2)$$

$$H_t = - \sum_{\kappa=1,4} t_{\kappa} \sum_{\langle i,j \rangle \in D_{\kappa,\sigma}} \hat{c}_{i,\sigma}^{\dagger} \hat{c}_{j,\sigma} + H.c., \quad (3)$$

with $\hat{c}_{i,\sigma}^{(\dagger)} = [c_{i,\sigma}(1 - n_{i,-\sigma})]^{(\dagger)}$, where $c_{i,\sigma}^{(\dagger)}$ annihilates (creates) an electron and $n_{i,\sigma}$ is the electron number with spin σ ($=\uparrow, \downarrow$) at the i th site. The corresponding spin operator is defined by $\mathbf{S}_i = \frac{1}{2} \sum_{\sigma,\sigma'} c_{i,\sigma}^{\dagger} \boldsymbol{\tau}_{\sigma,\sigma'} c_{i,\sigma'}$, where $\boldsymbol{\tau}$ is the Pauli matrix. We introduce four types of hopping integrals $t_{\kappa} > 0$ and exchange couplings

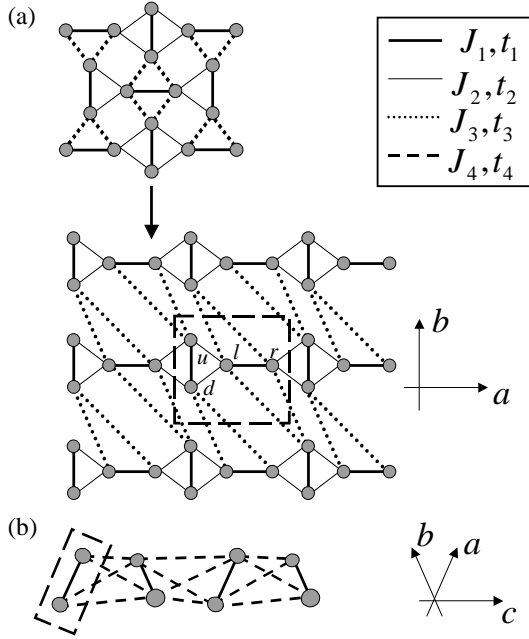


Fig. 1. Orthogonal-dimer system for $\text{SrCu}_2(\text{BO}_3)_2$, which has alternating orthogonal-dimers in all directions along the a , b and c axes: (a) the 2D Shastry-Sutherland model in the a - b plane. Square unit cell containing four spins is shown as a long dashed line. If we set $J_3 = t_3 = 0$ (dotted line), the system is reduced to an orthogonal-dimer chain with alternating dimer-plaquette structure; (b) configuration of the dimers along the c -axis, which forms another type of orthogonal-dimer chain. This is equivalent to a ladder model with additional exchange interactions for diagonal bonds, which is referred to as tetrahedra chain.

$J_\kappa > 0$ ($\kappa = 1, 2, 3, 4$), which are specified by the bond pairs $D_\kappa = \{J_\kappa, t_\kappa\}$ shown in Fig. 1. Note that this generalized model has the orthogonal-dimer structure in all three directions, thereby allowing us to discuss the hole doping effect systematically in one, two and three dimensions. When $J_2 = J_3$ and $J_4 = 0$, the system is reduced to the well-known 2D Shastry-Sutherland model,⁹⁾ static properties of which have been intensively studied so far.^{8, 11–24, 26–28)} The system is further reduced to a 1D orthogonal-dimer system if we consider the chain system along the a or b axis (lower panel of Fig. 1(a)). Also, the 1D system along the c axis forms another orthogonal-dimer chain, as shown in Fig. 1(b). Magnetic properties of these chain models have been studied in detail.^{44–47, 49, 50, 50–55)}

In contrast to well-studied static properties, systematic investigation of one-particle spectral properties³¹⁾ is still lacking, which we will address in the following sections.

3. Bond operator approach

In this section, we introduce a method to treat the dynamics of a doped hole. Since we are mainly concerned with the dimer phase, it is convenient to use the bond operator representation,^{31, 37–41)} which may describe the ground state as well as low-energy excitations in the dimer phase rather well. The essence of this method is to represent the Hamiltonian in terms of "bond operators", which act on each dimer pair formed by J_1 , instead

of original operators for spins and electrons. Since the generalized Shastry-Sutherland model has four sites in a unit cell, we introduce the bond operators defined as,

$$\begin{aligned}
 s_n^\dagger |0\rangle &= \frac{1}{\sqrt{2}}(|\uparrow\downarrow\rangle - |\downarrow\uparrow\rangle) \\
 t_{x,n}^\dagger |0\rangle &= \frac{-1}{\sqrt{2}}(|\uparrow\uparrow\rangle - |\downarrow\downarrow\rangle) \\
 t_{y,n}^\dagger |0\rangle &= \frac{i}{\sqrt{2}}(|\uparrow\uparrow\rangle + |\downarrow\downarrow\rangle) \\
 t_{z,n}^\dagger |0\rangle &= \frac{1}{\sqrt{2}}(|\uparrow\downarrow\rangle + |\downarrow\uparrow\rangle) \\
 a_{u,n,\sigma}^\dagger |0\rangle &= |\sigma, \circ\rangle_n, \\
 a_{d,n,\sigma}^\dagger |0\rangle &= |\circ, \sigma\rangle_n,
 \end{aligned} \tag{4}$$

for a vertical bond and

$$\begin{aligned}
 s'_n |0\rangle &= \frac{1}{\sqrt{2}}(|\uparrow\downarrow\rangle - |\downarrow\uparrow\rangle) \\
 p_{x,n}^\dagger |0\rangle &= \frac{-1}{\sqrt{2}}(|\uparrow\uparrow\rangle - |\downarrow\downarrow\rangle) \\
 p_{y,n}^\dagger |0\rangle &= \frac{i}{\sqrt{2}}(|\uparrow\uparrow\rangle + |\downarrow\downarrow\rangle) \\
 p_{z,n}^\dagger |0\rangle &= \frac{1}{\sqrt{2}}(|\uparrow\downarrow\rangle + |\downarrow\uparrow\rangle), \\
 a_{l,n,\sigma}^\dagger |0\rangle &= |\sigma, \circ\rangle_n, \\
 a_{r,n,\sigma}^\dagger |0\rangle &= |\circ, \sigma\rangle_n,
 \end{aligned} \tag{5}$$

for a horizontal bond at the n -th cluster in Fig. 1. The operators $s(s')$, $t_\alpha(p_\alpha)$ ($\alpha = x, y, z$) obey the bosonic commutation relation, while the operator a the fermionic anticommutation relation. The notations u, d, l, r specify the *up*, *down*, *left* and *right* sites in the unit cell as shown in the lower panel of Fig. 1(a). The ket states are labeled by the configuration of electrons sitting at up (left) and down (right) sites of the vertical (horizontal) bond [\circ represents an unoccupied (hole) site]. To restrict the Hilbert space to the physically sensible one, we introduce the following constraints,

$$s_n^\dagger s_n + \sum_\alpha t_{\alpha,n}^\dagger t_{\alpha,n} + \sum_{\sigma, i=u,d} a_{i,n,\sigma}^\dagger a_{i,n,\sigma} = 1, \tag{6}$$

$$s'_n s'_n + \sum_\alpha p_{\alpha,n}^\dagger p_{\alpha,n} + \sum_{\sigma, i=l,r} a_{i,n,\sigma}^\dagger a_{i,n,\sigma} = 1. \tag{7}$$

We are now considering the dimer phase for the host spin system, which is realized by the condensation of the singlet-bond operators, s_n and s'_n . The remaining triplet operators describe spin excitations in the host system, giving H_J in the Fourier space,

$$\begin{aligned}
 H_J &= -\frac{3}{2} J_1 N \\
 &+ \sum_{\mathbf{k}, \alpha} \{ \omega_{1\mathbf{k}} t_{\alpha,\mathbf{k}}^\dagger t_{\alpha,\mathbf{k}} + \omega_{2\mathbf{k}} p_{\alpha,\mathbf{k}}^\dagger p_{\alpha,\mathbf{k}} \}
 \end{aligned} \tag{8}$$

with

$$\begin{aligned} t_{\alpha,i}^\dagger &= \sqrt{\frac{1}{N}} \sum_{\mathbf{k}} t_{\alpha,\mathbf{k}}^\dagger e^{i\mathbf{k}\mathbf{r}_i}, \\ p_{\alpha,i}^\dagger &= \sqrt{\frac{1}{N}} \sum_{\mathbf{k}} p_{\alpha,\mathbf{k}}^\dagger e^{i\mathbf{k}\mathbf{r}_i}, \end{aligned} \quad (9)$$

where $\omega_{1k} = \omega_{2k} = J_1$, N is the number of unit cells and \mathbf{k} is the wave vector. When we have derived the Hamiltonian (8), the interactions among triplets have been discarded due to their minor importance. We note that the triplet excitations ω_1 and ω_2 obtained do not depend on the wave number, implying that the orthogonal-dimer structure forbids the motion of the triplet. In fact, it is known that the triplet excitation does not have the dispersion up to the fifth order in the inter-dimer coupling for the 2D model.⁸⁾ To make our discussions more quantitative, we use the triplet excitation energy obtained by the perturbation expansion up to the fourth order,

$$\begin{aligned} \omega_{1k} &= J_1 \left\{ 1 - \left(\frac{J_2}{J_1}\right)^2 - \frac{1}{2} \left(\frac{J_2}{J_1}\right)^3 \right. \\ &\quad \left. + \frac{3}{8} \left(\frac{J_2}{J_1}\right)^4 - \frac{1}{2} \left(\frac{J_3}{J_1}\right)^2 \left(\frac{J_2}{J_1}\right)^2 \right\} \end{aligned} \quad (10)$$

$$\begin{aligned} \omega_{2k} &= J_1 \left\{ 1 - \left(\frac{J_3}{J_1}\right)^2 - \frac{1}{2} \left(\frac{J_3}{J_1}\right)^3 \right. \\ &\quad \left. + \frac{3}{8} \left(\frac{J_3}{J_1}\right)^4 - \frac{1}{2} \left(\frac{J_2}{J_1}\right)^2 \left(\frac{J_3}{J_1}\right)^2 \right\}. \end{aligned} \quad (11)$$

We now consider the hole dynamics in the orthogonal-dimer system. To this end, we define the retarded Green function for physical fermions in the 4×4 matrix form,

$$G_\sigma(\mathbf{k}, t) = -i\Theta(t)\langle D | \{ \phi_{\mathbf{k},\sigma}(t), \phi_{\mathbf{k},\sigma}^\dagger \} | D \rangle, \quad (12)$$

where $\phi_{\mathbf{k},\sigma}^\dagger = (\hat{c}_{u,\mathbf{k},\sigma}^\dagger, \hat{c}_{d,\mathbf{k},\sigma}^\dagger, \hat{c}_{r,\mathbf{k},\sigma}^\dagger, \hat{c}_{l,\mathbf{k},\sigma}^\dagger)$ and $|D\rangle$ is the dimer singlet ground state.⁸⁾ We employ here the SCBA to obtain the self-energy of the Green functions. It is known that this approximation works rather well as far as a single hole doped in quantum spin systems is concerned.³³⁻³⁸⁾ Following standard procedures in the SCBA, we compute the spectral function of the physical fermion defined by

$$A(\mathbf{k}, \omega) = -\frac{1}{\pi} \text{Im Tr } G(\mathbf{k}, \omega), \quad (13)$$

which directly gives the photoemission spectrum. This function satisfies the sum rule, $\int A(\mathbf{k}, \omega) d\omega = 2$.

This completes the formulation of the bond-operator treatment of the dimer phase. We will also employ the ED calculation of the finite-size system to check the validity of the bond-operator approach. Moreover, we will see that the latter ED calculation is efficient to discuss the hole dynamics in another singlet phase of the model, i.e. the plaquette phase.

Here we make a comment on the exchange couplings of our generalized model. If we consider the t - J model (1) is to be derived from a strong-coupling limit of the Hubbard model with on-site repulsion U , the ratio of the

parameters is given as,

$$\frac{t_1^2}{J_1} = \frac{t_2^2}{J_2} = \frac{t_3^2}{J_3} = \frac{t_4^2}{J_4} = \frac{U}{4}. \quad (14)$$

We use these relations when the ratio of the exchange coupling and hopping is altered.

4. Hole dynamics in orthogonal-dimer system

4.1 orthogonal-dimer chain

We begin with the 1D spin chain ($J_3 = J_4 = 0$) shown in the lower panel of Fig. 1(a), which may have essential properties inherent in the orthogonal-dimer systems.^{44-47,50)} Before presenting the computed results, we note that the ground state of the chain model belongs to the dimer (plaquette) singlet phase for $J_2/J_1 < J_c (> J_c)$ with $J_c = 0.819$.⁴⁴⁻⁴⁷⁾ Shown in Fig. 2 is the spectral function $A(\mathbf{k}, \omega)$ for the dimer phase, which has been calculated by combining the bond operator method with the SCBA. Since there are four sites in the unit cell,

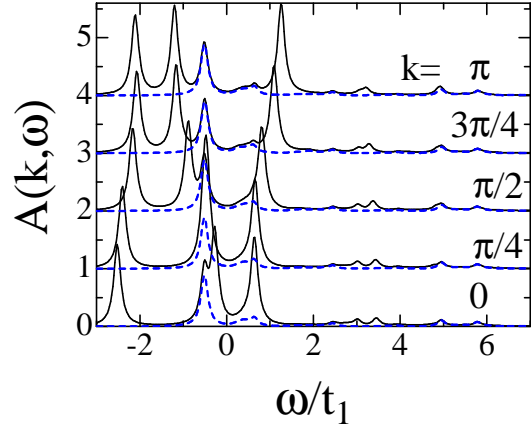


Fig. 2. Spectral function $A(\mathbf{k}, \omega)$ for the orthogonal-dimer chain with $J_1 = 5$, $J_2 = 5 \times 0.635$ and $J_3 = J_4 = 0$ (dimer phase). The contribution of the dispersionless mode is shown by the dashed line.

we have four kinds of clear peaks in the spectral function: three dispersive modes and one dispersionless mode. We refer to the lowest mode having clear dispersion as the quasi-particle state. We thus say that the quasi-particle state is well defined and is mobile rather freely in the background of the dimer singlets.

In the plaquette phase, the spectral function $A(\mathbf{k}, \omega)$ shows a similar four-peak structure, as seen in Fig. 3, which is obtained by the ED calculation of the finite system ($J_1 = 5$, $J_2 = 5 \times 0.85$). In this case, however, the lowest quasi-particle peak is dispersionless, in contrast to the dimer phase, implying that a doped hole is forbidden to itinerate in the chain system. This results in a completely localized quasi-particle state.

We now clarify why the above characteristic features appear in the spectral function, by taking into account symmetry property inherent in the orthogonal-dimer structure. This consideration may be also helpful to discuss the 2D and 3D cases. Notice first that the system has symmetry of space inversion P for each vertical dimer-pair; namely if the pair forms a singlet (triplet), we have the eigenvalue $P = 1$ ($P = -1$). Then, the

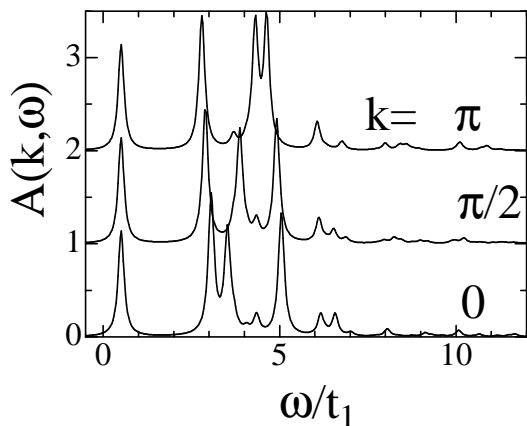


Fig. 3. Spectral function $A(\mathbf{k}, \omega)$ for the chain in the plaquette phase ($J_1 = 5$, $J_2 = 5 \times 0.85$) obtained by the ED for the small system (16 sites).

Hilbert space of the Hamiltonian is classified into each subspace specified by a set of the eigenvalues $\{P_i\}$. In the dimer (plaquette) phase for the undoped case, the singlet (triplet) state is realized on every vertical bond.⁴⁷⁾ Therefore the ground state of these phases is respectively given by the lowest state in the subspaces $[111 \dots]$ and $[\bar{1}\bar{1}\bar{1} \dots]$, as shown in Fig. 4(a).

Now consider the hole doping effect. In the dimer phase, a certain dimer singlet may be broken by a doped hole, but the bonding state (symmetric superposition) is formed between the doped hole and the corresponding unpaired spin. Therefore the ground state in the doped case is still in the same subspace $[111 \dots]$, since the bonding state on a vertical bond has the eigenvalue $P = 1$ (Fig. 4(b)). This symmetry property renders the hole state mobile, making a well defined quasi-particle state. Two other dispersive modes in Fig. 2 belong to this class of $P = 1$. On the other hand, a dispersionless hole state is realized by creating an anti-bonding state ($P = -1$) at a broken-dimer site, which thus belongs to the subspace $[\bar{1}\bar{1}\bar{1} \dots]$. Since the different inversion symmetry between neighboring pairs prohibits the motion of a hole, leading to a completely-localized excited state.

Similar consideration can be applied to the hole doping in the plaquette phase. In this case, however, the energy level of the anti-bonding hole state ($P = -1$) is higher than that for the bonding state ($P = 1$). Therefore, the ground state is not realized in the subspace of $[\bar{1}\bar{1}\bar{1} \dots]$ but in $[\bar{1}1\bar{1} \dots]$, as indeed seen in Fig. 4(b). Therefore, we end up with a completely-localized quasi-particle (lowest-energy) state upon hole doping in the plaquette phase.

4.2 2D Shastry-Sutherland model

We now turn to the 2D case. In the following, we discuss how the spectral function of a doped hole is changed when the interchain coupling J_3 is introduced. We begin with a quasi-particle state in the dimer phase. The spectral function obtained by the SCBA is shown in Fig. 5. It is seen that the introduction of the interchain coupling increases the band width of the lowest mode while

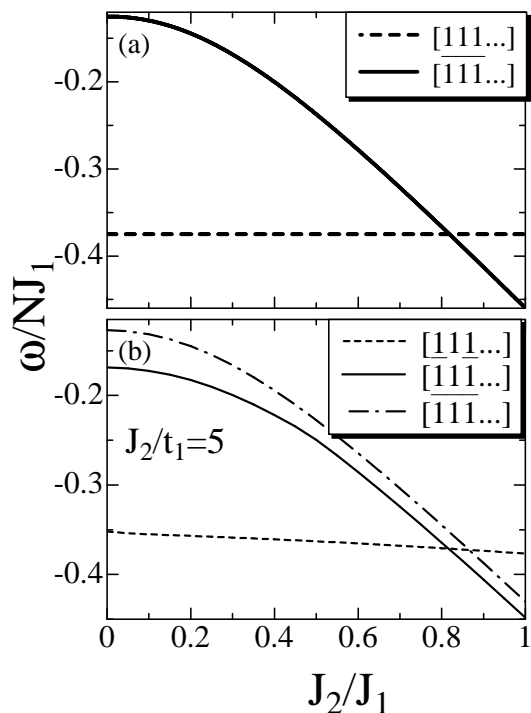


Fig. 4. The energy of the lowest state in the distinct subspaces (a) undoped case, (b) one-hole case. The data are obtained by the ED for the system (24 sites) with periodic boundary conditions.

keeping its dispersive peak. This implies that the quasi-particle state is well defined even in the 2D Shastry-Sutherland model, in accordance with the results of Vojta.³¹⁾ On the other hand, other peaks in the high energy region are considerably smeared with increase of the interchain coupling. Such smearing effects are induced by scattering by triplet bosons.

Now let us turn to the plaquette phase. Note that this type of plaquette-singlet phase may exist even in the 2D Shastry-Sutherland model due to strong frustration, which is believed to be sandwiched by the dimer phase and the antiferromagnetically ordered phase.^{11, 18, 19)} We discuss here the dynamical properties of the doped hole in the plaquette phase. By using the ED calculation of the 4×4 small cluster, we obtain the spectral function as shown in Fig. 6. The introduction of the interchain coupling J_3 has little effect on the quasi-particle state (lowest-energy state) except for the simple energy shift. In particular, it should be noticed that the dispersionless quasi-particle state can persist even in the 2D system. We also note that higher dispersive peaks are not so much smeared in comparison with those in the dimer phase. This is partially due to the finite-size calculation we have used for the plaquette phase.

For reference, we plot the band width of the quasi-particle state in Fig. 7. In the dimer phase, the band width is roughly proportional to hopping t , and thus it increases in proportion to the square root of J_2/J_1 since the ratio of hopping and exchange coupling is fixed as in eq. (14). At the critical point J_c , the band width shows discontinuity, reflecting the first-order quantum phase transition. Beyond the critical point J_c , the doped hole hardly itinerates, as mentioned above. In particular,

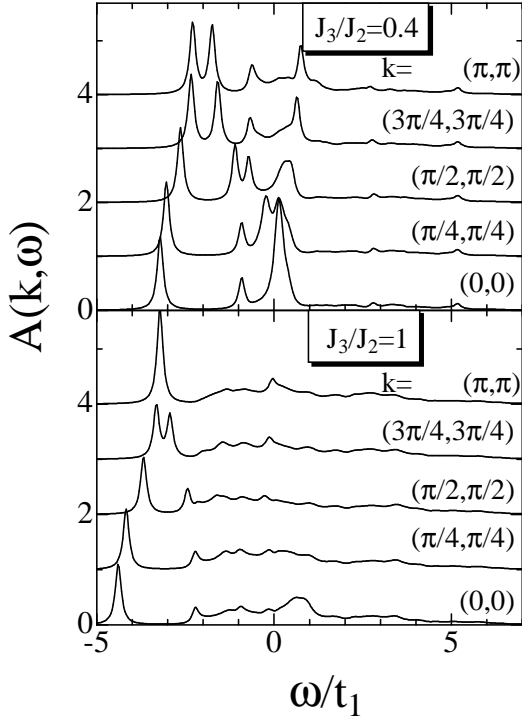


Fig. 5. Spectral function $A(\mathbf{k}, \omega)$ in the dimer phase ($J_1 = 5$ and $J_2 = J_1 \times 0.635$).

in the chain case ($J_3 = 0$), it is completely localized. By increasing the interchain coupling J_3 , the doped hole can itinerate in the system even for the plaquette phase, giving rise to a slight increase of the band width.

Summarizing the above results, we can say that the one-particle (photo-emission) spectrum provides an efficient probe to distinguish the two spin-gap phases clearly; i.e. a dispersive (almost localized) quasi-particle state characterizes the dimer (plaquette) phase. We wish to note that similar behavior appears in a triplet spin excitation spectrum in the undoped case, for which characteristic properties in the two phases are interchanged. Namely, a triplet excitation forms a completely localized (dispersive) mode for the dimer (plaquette) phase in the 1D case. Even in 2D, it has been shown that a triplet excitation in the dimer phase is almost localized.⁸⁾ Therefore, we can efficiently use these properties to analyze the photoemission spectrum and/or the neutron scattering experiments to figure out whether a plaquette phase can be really realized experimentally by changing the pressure, the magnetic field, etc.

4.3 Effects of the interlayer coupling

Finally, we discuss to what extent the above characteristic properties can persist in the presence of the inter-layer coupling. Some recent reports claimed that the compound $\text{SrCu}_2(\text{BO}_3)_2$ has rather large interlayer couplings, which may not be negligible to explain the experimental findings.^{12,30)} Nevertheless, it is known that some of physical quantities can be explained rather well by the 2D model. We address this question on the hole dynamics in the quasi-2D orthogonal-dimer system. We are mainly concerned with the dimer phase below in this

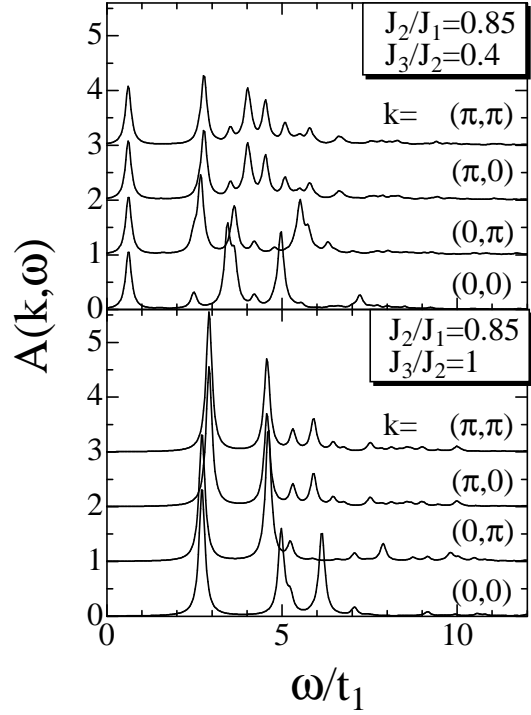


Fig. 6. Spectral function $A(\mathbf{k}, \omega)$ in the plaquette phase. The choice of the parameters are $J_1 = 5$ and $J_2 = J_3 = J_1 \times 0.85$, for which the plaquette singlet phase should be stabilized.^{11,18,19)}

section.

We show the computed spectral function of a doped hole in the quasi-2D case in Fig. 8, where we have chosen two different interlayer couplings $J_4/J_1 = 0.09$ and 0.2 with fixed $J_2/J_1 = J_3/J_1 = 0.635$. A remarkable point is that the introduction of the interlayer couplings J_4 and t_4 does not obscure the spectral function, and seems to even sharpen its characteristic peak structure in some energy region. We show below that this remarkable behavior is caused by the specific arrangement of dimers in the direction along the c -axis.

To make this point clear, we exploit a simplified model of the two-leg ladder with diagonal bonds, which is the basic structure along the c -direction (see Fig. 1 (b)). Magnetic properties of this ladder model have been al-

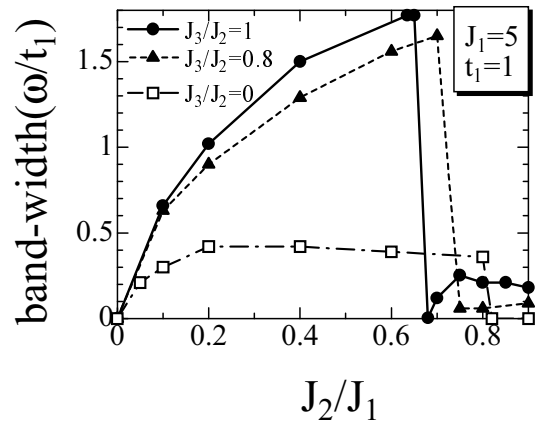


Fig. 7. Band-width of the lowest energy band (quasi-particle state) as a function of J_2/J_1 with J_3/J_2 being fixed.

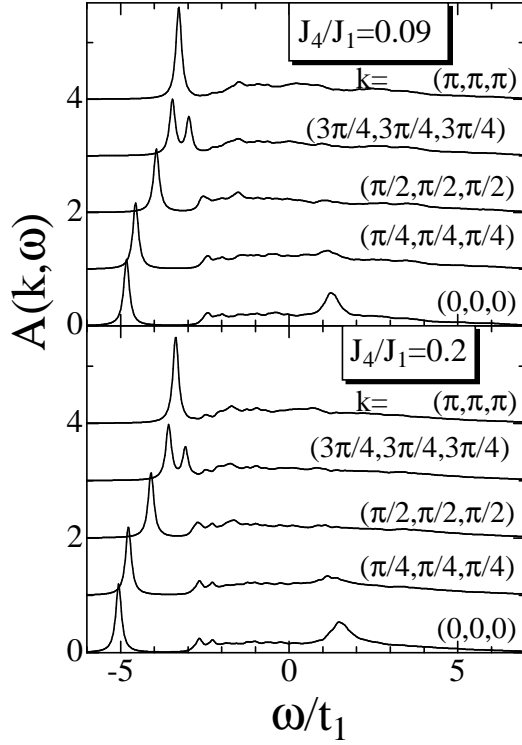


Fig. 8. Spectral function $A(\mathbf{k}, \omega)$ in the dimer phase ($J_1 = 5$ and $J_2 = J_3 = J_1 \times 0.635$) with the interlayer coupling $J_4 = J_1 \times 0.09$ and $J_4 = J_1 \times 0.2$. Both choices belong to the dimer phase.

ready studied in detail.^{49–55} To analyze the hole dynamics in this ladder system, it is convenient to introduce the fermionic operators for bonding and antibonding hole states, which are defined as

$$\begin{aligned} a_{s,\sigma,n}^\dagger &= \frac{1}{\sqrt{2}}(a_{2,\sigma,n}^\dagger + a_{1,\sigma,n}^\dagger), \\ a_{a,\sigma,n}^\dagger &= \frac{1}{\sqrt{2}}(a_{2,\sigma,n}^\dagger - a_{1,\sigma,n}^\dagger). \end{aligned} \quad (15)$$

Here the fermionic operators $a_{1,\sigma,n}$ and $a_{2,\sigma,n}$ denote hole states created at two distinct sites of the n -th rung in the c -direction. These two states span two independent Hilbert spaces when the hopping and the exchange couplings are introduced along the c -direction. The Hamiltonian for the bonding hole state is immediately diagonalized, and the corresponding eigenstate and the eigenvalue are given as,

$$|\psi_{s,\sigma,k}\rangle = \frac{1}{\sqrt{N'}} \sum_n \exp(ikn) a_{s,\sigma,n}^\dagger s_n |D\rangle, \quad (16)$$

$$\epsilon_k = t_1 - 2t_4 \cos k, \quad (17)$$

where N' is the number of unit cells. An important point is that the doped hole in a bonding (symmetric) state can move in the ladder *without producing any triplet excitations*. This is a strong constraint coming from local symmetry due to the unique dimer alignment in the c -direction. Therefore, the quasi-particle peak appears clearly in Fig. 9. On the other hand, an anti-bonding (anti-symmetric) hole state a_a is completely localized, as shown in Fig. 9. We have also confirmed this conclu-

sion by calculating the spectral function by the ED for the small cluster $N' = 8$, which is shown in Fig. 9 by the dashed line. It is seen that the results show good agreement with those obtained by the SCBA.

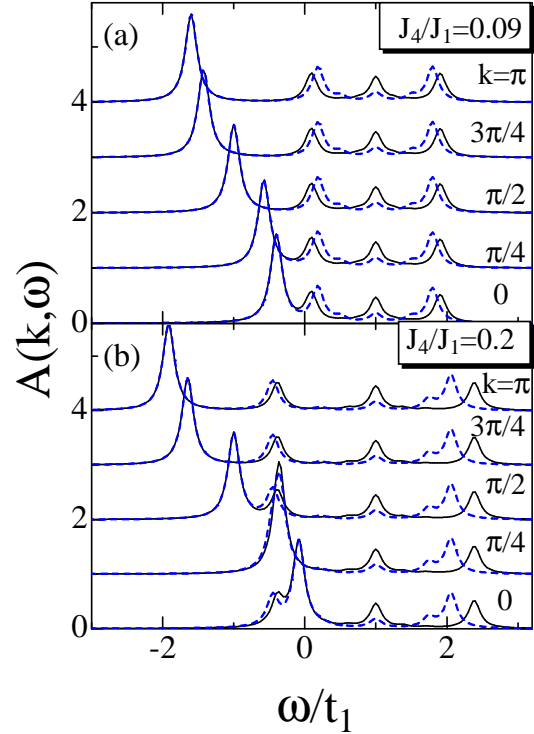


Fig. 9. Spectral function of tetrahedra chain. (a) $J_1 = 2$ and $J_4 = J_1 \times 0.09$ (b) $J_1 = 2$ and $J_4 = J_1 \times 0.2$. The dashed line represents the results obtained by the ED.

The above analysis is valid for the ladder system, but most of essential features may appear even in the quasi-2D case along the c -direction although the profile of the spectrum may be somewhat obscured. This naturally explains why the quasi-particle peak in the low energy region in the orthogonal-dimer system is not smeared by the interlayer coupling.

To conclude this section, we check how well the quasi-particle state is stabilized in 3D by estimating the quasi-particle weight defined by

$$Z(\mathbf{k}) = \left(1 - \text{Re} \frac{\partial \Sigma(\mathbf{k}, \omega)}{\partial \omega} \right)^{-1} \Big|_{\omega=\epsilon_{\mathbf{k}}}, \quad (18)$$

where $\epsilon_{\mathbf{k}}$ is the energy of the quasi-particle. Shown in Fig. 10 is the weight computed at the Γ point when the ratio of the exchange coupling and the hopping is varied. In the parameter region shown in the figure, there are two characteristic features. (i) the change in character from 1D to 2D: By comparing the data of $J_3 = J_4 = 0$ (dotted line) with those of $J_4 = 0$ (broken line), we notice that the increase of the interchain coupling results in the decrease of the quasi-particle weight in accordance with the discussions given above. (ii) Change from 2D to 3D: On the other hand, the increase of the inter-layer coupling does not lead to the decrease of the weight, but has a tendency to increase it, as seen from the solid and dash-dotted lines in Fig. 10. This property is related to the fact that the motion of a hole in the c -direction is

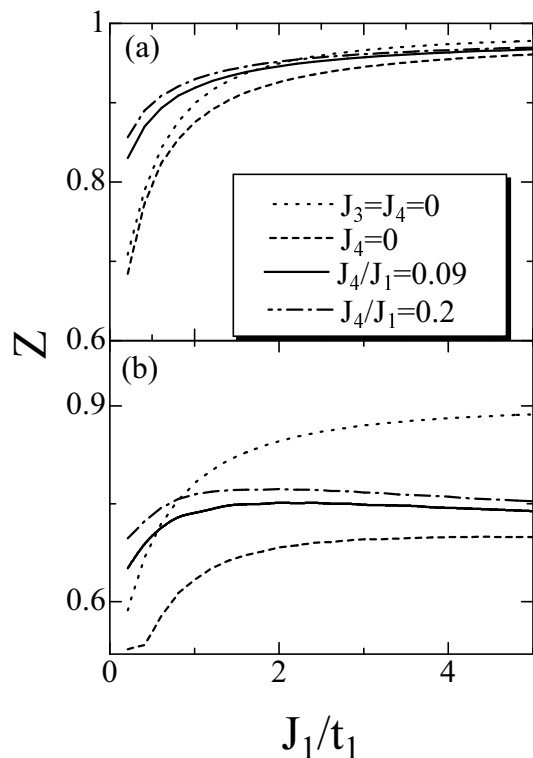


Fig. 10. Renormalization factor at the Γ point with (a) $J_2/J_1 = J_3/J_1 = 0.2$ and (b) $J_2/J_1 = J_3/J_1 = 0.635$.

quite free, rendering the quasi-particle state more stable.

5. Summary

We have investigated the hole dynamics in the orthogonal-dimer model proposed for the quasi-2D compound $\text{SrCu}_2(\text{BO}_3)_2$. In particular, the characteristic properties present in the one-particle spectrum have been clarified in detail, by systematically studying the one, two and three dimensional systems. We have demonstrated that the quasi-particle state of a doped hole is well stabilized due to the specific orthogonal-dimer structure. Furthermore, it has been found that the one-particle spectral function provides an efficient way to distinguish the two spin-gap phases; i.e. a dispersive (almost localized) quasi-particle mode characterizes the dimer (plaquette) phase. This remarkable property is inherent in the orthogonal-dimer system, which stems from a strong constraint due to local symmetry.

We expect that the plaquette singlet phase could be realized experimentally by applying the pressure or the chemical pressure with substitution of certain elements. In order to judge which type of spin-gap phase is realized in such case, an efficient probe is necessary to distinguish them properly. We have found here that the photoemission spectrum can be an efficient method to specify the nature of the spin-gap phases.

6. Acknowledgments

Our ED computational programs are based on TITPACK, Version 2, by Nishimori. This work was partly supported by a Grant-in-Aid from the Ministry of Ed-

ucation, Science, Sports and Culture of Japan. A part of calculations was done at the Supercomputer Center at the Institute for Solid State Physics, University of Tokyo.

- 1) H. Kageyama, K. Yosimura, R. Stern, N. V. Mushnikov, K. Onizuka, M. Kato, K. Kosuge, C. P. Slichter, T. Goto and Y. Ueda, Phys. Rev. Lett. **82**, 3168 (1999).
- 2) K. Kodama, M. Takigawa, M. Horovatic, C. Berthier, H. Kageyama, Y. Ueda, S. Miyahara, F. Becca and F. Mila, Science **298** 395 (2002)
- 3) K. Onizuka, H. Kageyama, Y. Narumi, K. Kindo, Y. Ueda and T. Goto, J. Phys. Soc. Jpn. **69**, 1016 (2000).
- 4) N. Aso, H. Kageyama, K. Nukui, M. Nishi, K. Kakurai, K. Onizuka, Y. Ueda, and H. Kadowaki, to be published in J. Phys. Chem. Solid. (2002)
- 5) H. Nojiri, H. Kageyama, K. Onizuka, Y. Ueda and M. Motokawa, J. Phys. Soc. Jpn. **68**, 2906 (1999).
- 6) P. Lemmens, M. Grove, M. Fischer, G. Güntherodt, V. N. Kotov, H. Kageyama, K. Onizuka and Y. Ueda, Phys. Rev. Lett. **85**, 2605 (2000).
- 7) H. Kageyama, N. V. Mushnikov, M. Yamada, T. Goto and Y. Ueda, Physica B **329**, 1020 (2003).
- 8) S. Miyahara and K. Ueda, Phys. Rev. Lett. **82**, 3701 (1999).
- 9) B. S. Shastry and B. Sutherland, Physica B **108**, 1069 (1981).
- 10) S. Miyahara and K. Ueda, J. Phys: Condens. Matter **15**, R327-R366 (2003)
- 11) A. Koga and N. Kawakami, Phys. Rev. Lett. **84**, 4461 (2000).
- 12) C. Knetter, A. Bühler, E. Müller – Hartmann and G. S. Uhrig, Phys. Rev. Lett. **85**, 3958 (2000)
- 13) Z. Weihong, C. J. Harmer and J. Oitmaa, Phys. Rev. B **60**, 6608 (1999); Phys. Rev. B **65**, 014408 (2002).
- 14) E. Müller – Hartmann, R. R. P. Singh, C. Knetter and G. Uhrig, Phys. Rev. Lett. **84**, 1808 (2000).
- 15) M. Albrecht and F. Mila, Europhys. Lett. **34**, 145 (1996)
- 16) C. H. Chung, J. B. Marston and S. Sachdev, Phys. Rev. B **64**, 134407 (2001).
- 17) D. Carpentier and L. Balents, Phys. Rev. B **65**, 024427 (2002).
- 18) Y. Takushima, A. Koga and N. Kawakami, J. Phys. Soc. Jpn. **70**, 1369 (2000).
- 19) A. Läuchli, S. Wessel and M. Sigrist Phys. Rev. B **66**, 014401 (2002).
- 20) K. Totsuka, S. Miyahara and K. Ueda, Phys. Rev. Lett. **86**, 520 (2001).
- 21) T. Momoi and K. Totsuka, Phys. Rev. B **61**, 3231 (2000); Phys. Rev. B **62**, 15067 (2000).
- 22) K. Totsuka, S. Miyahara and K. Ueda, Phys. Rev. Lett. **86**, 520 (2000)
- 23) Y. Fukumoto, J. Phys. Soc. Jpn. **69**, 2755 (2000).
- 24) C. Knetter and G. Uhrig, cond-mat/0309408.
- 25) T. Munehisa and Y. Munehisa, J. Phys. Soc. Jpn. **69**, 1286 (2000).
- 26) S. Miyahara and K. Ueda, Phys. Rev. B **61**, 3417 (2000).
- 27) G. Misguich, Th. Jolicoeur and S. M. Girvin, Phys. Rev. Lett. **27**, 097203 (2001)
- 28) Y. Fukumoto and A. Oguchi, J. Phys. Soc. Jpn. **69**, 1286 (2000).
- 29) S. Miyahara, F. Becca and F. Mila, Phys. Rev. B **68**, 024401 (2003).
- 30) S. Miyahara and K. Ueda, J. Phys. Soc. Jpn. Suppl. B **69**, 72 (2000).
- 31) M. Vojta, Phys. Rev. B **61**, 11309 (2000).
- 32) H. Kageyama, Y. Narumi, K. Kindo, K. Onizuka, Y. Ueda, and T. Goto, J. Alloys and Compounds **317-318**, 177-182 (2001).
- 33) S. Schmitt-Rink, C. M. Varma and A. E. Ruckenstein, Phys. Rev. Lett. **60**, 2793 (1988).
- 34) G. Martinez and P. Horsh, Phys. Rev. B **44**, 317 (1991).
- 35) Z. Liu and E. Manousakis, Phys. Rev. B **45**, 2425 (1992).
- 36) F. Magsiglio, A. Ruckenstein, Schmitt-Rink and C. Varma, Phys. Rev. B **43**, 10882 (1991).
- 37) C. Jurecka and W. Brenig, Phys. Rev. B **63**, 094409 (2001).
- 38) Y. Saito, A. Koga and N. Kawakami J. Phys. Soc. Jpn. **72**, 60349 (2003).
- 39) S. Sachdev and N. Bhatt, Phys. Rev. B **41**, 9323 (1990).
- 40) S. Gopalan, T. M. Rice and M. Sigrist, Phys. Rev. B **49**, 8901

- (1994).
- 41) M. Matsumoto, B. Normand, T. M. Rice and M. Sigrist, Phys. Rev. Lett. **89**, 077203 (2002)
- 42) K. Ueda and S. Miyahara, J. Phys. Condens. Matter. **11** L175 (1999).
- 43) A. Koga, J. Phys. Soc. Jpn. **69**, 3509 (2000).
- 44) N. B. Ivanov and J. Richter, Phys. Lett. A **232**, 308 (1997).
- 45) J. Schulenburg and J. Richter, Phys. Rev. B **65**, 054420 (2002); Phys. Rev. B **66**, 134419 (2002).
- 46) J. Richter, N. B. Ivanov and J. Schulenburg, J. Phys. Condens. Matter. **10** 3635 (1998).
- 47) A. Koga, K. Okunishi and N. Kawakami, Phys. Rev. B **62**, 5558 (2000); Phys. Rev. B **65**, 214415 (2002).
- 48) A. Honecker, J. Schulenburg and J. Richter, cond-mat/0309425.
- 49) M. P. Gelfand, Phys. Rev. B **43**, 8644 (1991).
- 50) A. Honecker, F. Mila and M. Troyer, Eur. Phys. J. B. **15**, 227 (2000).
- 51) W. Brenig and K. W. Becker, Phys. Rev. B **64**, 214413 (2001).
- 52) E. H. Kim, G. Fáth, J. Sólyom and D. J. Scalapino, Phys. Rev. B **62**, 14965 (2000).
- 53) K. Totsuka and H.-J. Mikeska, Phys. Rev. B **66**, 054435 (2002).
- 54) B. Sutherland, Phys. Rev. B **62**, 11499 (2000).
- 55) A. Kawaguchi, A. Koga, K. Okunishi and N. Kawakami J. Phys. Soc. Jpn. **72**, 405 (2003).